


Article

Phanerosides A–X, Phenylpropanoid Esters of Sucrose from the Rattans of *Phanera championii* Benth

Ya-Jie Hu [†], Qian Lan [†], Bao-Jun Su and Dong Liang ^{*} 

State Key Laboratory for Chemistry and Molecular Engineering of Medicinal Resources, Collaborative Innovation Center for Guangxi Ethnic Medicine, School of Chemistry and Pharmaceutical Sciences, Guangxi Normal University, Guilin 541004, China

* Correspondence: liangdong@mailbox.gxnu.edu.cn or liangdonggxnu@163.com

[†] These authors contributed equally to this work.

Abstract: Twenty-four new phenylpropanoid esters of sucrose, phanerosides A–X (1–24), were isolated from an EtOH extract of the rattans of *Phanera championii* Benth. (Fabaceae). Their structures were elucidated on the basis of comprehensive spectroscopic data analysis. A wide range of structural analogues were presented due to the different numbers and positions of acetyl substituents and the structures of phenylpropanoid moieties. Phenylpropanoid esters of sucrose were isolated from the Fabaceae family for the first time. Biologically, the inhibitory effects of compounds 6 and 21 on NO production in LPS-induced BV-2 microglial cells were better than that of the positive control, with IC₅₀ values of 6.7 and 5.2 μM, respectively. The antioxidant activity assay showed that compounds 5, 15, 17, and 24 displayed moderate DPPH radical scavenging activity, with IC₅₀ values ranging from 34.9 to 43.9 μM.

Keywords: *Phanera championii* Benth.; Fabaceae; phenylpropanoid esters of sucrose; anti-inflammatory; antioxidant



Citation: Hu, Y.-J.; Lan, Q.; Su, B.-J.; Liang, D. Phanerosides A–X, Phenylpropanoid Esters of Sucrose from the Rattans of *Phanera championii* Benth. *Molecules* **2023**, *28*, 4767. <https://doi.org/10.3390/molecules28124767>

Academic Editors: Hang Ma, Chang Liu and Ang Cai

Received: 10 May 2023

Revised: 2 June 2023

Accepted: 5 June 2023

Published: 14 June 2023



Copyright: © 2023 by the authors. Licensee MDPI, Basel, Switzerland. This article is an open access article distributed under the terms and conditions of the Creative Commons Attribution (CC BY) license (<https://creativecommons.org/licenses/by/4.0/>).

1. Introduction

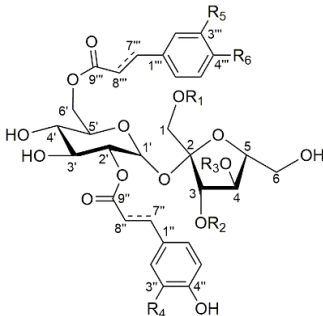
Phenylpropanoid esters of sucrose are characterized by the esterification of different hydroxy groups of sucrose with phenylpropanoid moieties [1,2]. These compounds have been isolated mainly from the families Arecaceae, Brassicaceae, Liliaceae, Polygonaceae, Rosaceae, Rutaceae, Smilacaceae, and Sparganiaceae [1,3]. The structural diversity of phenylpropanoid esters of sucrose generates extensive pharmacological antitumor [4–6], anti-inflammatory [7,8], antioxidant [9], an anti-HIV [10] activities, which are extremely thrilling to those engaged in medicinal chemistry [11,12].

Fabaceae is the third largest plant family, comprising approximately 800 genera and 20,000 species worldwide [13,14]. As the largest of the several genera in the Fabaceae family, *Phanera* results from the reorganization of *Bauhinia* sensu lato. The genus *Phanera* encompasses about 90–100 species, mainly distributed in tropical Asia and Australasia [15]. As one of them, *Phanera championii* Benth. is widely distributed in Guangxi Province and was first recorded in ‘Nanning Drug Chi’ [16]. It is a well-known folk medicine with a rich history of being used as medication to treat rheumatoid arthritis and epigastric pain [17,18]. Phytochemical investigations of this plant have primarily resulted in the isolation of flavonoids, nitrile glucoside, dibenzofurans, and diterpenoid [16,19–21]. In our ongoing research in pursuit of novel and biologically active metabolites from ethnic medicines in Guangxi, 24 new phenylpropanoid esters of sucrose (1–24) were isolated from the rattans of *P. championii*. Herein, the isolation, structural elucidation, anti-inflammatory, and antioxidant activities in vitro of all the isolated compounds are described.

2. Results and Discussion

Structural Elucidation

Compound **1** (Figure 1) was isolated as a white amorphous powder with a molecular formula of $C_{30}H_{34}O_{15}$, as determined using HRESIMS (m/z 657.1798 $[M + Na]^+$, calcd for 657.1790) and ^{13}C NMR data. The 1H NMR spectrum (Table 1) revealed two groups of AA'BB' aromatic signals [δ_H 7.49 (2H, d, $J = 8.8$ Hz, H-2''/6''), 6.82 (2H, d, $J = 8.8$ Hz, H-3''/5'') and 7.51 (2H, d, $J = 8.8$ Hz, H-2'''/6'''), 6.81 (2H, d, $J = 8.8$ Hz, H-3'''/5''')] and two sets of *trans*-olefinic protons [δ_H 7.72 (1H, d, $J = 16.0$ Hz, H-7''), 6.39 (1H, d, $J = 16.0$ Hz, H-8'') and 7.67 (1H, d, $J = 16.0$ Hz, H-7'''), 6.43 (1H, d, $J = 16.0$ Hz, H-8''')]. In addition, a characteristic doublet with a small coupling constant ($J = 3.6$ Hz) at δ_H 5.60 was also shown in the 1H NMR spectrum, which together with 12 oxygen-bearing carbon signals (including two anomers at δ_C 105.7 and 90.6) in the ^{13}C NMR data (Table 2) supposed the presence of a disaccharide moiety. Furthermore, detailed analysis of the 2D NMR correlations (Figure 2) and chiral HPLC analysis of monosaccharides after acid hydrolysis of **1** revealed that the two sugars were β -D-fructose and α -D-glucose units connected via C-2→C-1' to construct a D-sucrose moiety. The ^{13}C NMR spectrum showed 30 carbon signals, apart from the 12 carbon signals occupied by the D-sucrose moiety; the other 18 ones were classified as 2 carbonyl carbons (δ_C 169.2, 168.8) and 16 olefinic or aromatic carbons with the assistance of the HSQC data. Two discrete spin systems, H-7''/H-8'' and H-7'''/H-8''', in the 1H - 1H COSY spectrum, and the correlations from H-7'' to C-1''/C-2''/C-6''/C-9'' and H-7''' to C-1'''/C-2'''/C-6'''/C-9''' in the HMBC spectrum (Figure 2), established two *trans*-*p*-coumaroyl moieties. Subsequently, the key HMBC correlations from H-2' to C-9'' as well as from H-2' to C-9''' suggested that the two *trans*-*p*-coumaroyl moieties were located at C-2' and C-6'. Thus, the structure of **1** was identified and named phaneroside A.



	R ₁	R ₂	R ₃	R ₄	R ₅	R ₆	$\Delta^{7'',8''} E$	$\Delta^{7''',8'''} E$
1	H	H	H	H	H	OH	$\Delta^{7'',8''} E$	$\Delta^{7''',8'''} E$
2	H	H	H	H	H	H	$\Delta^{7'',8''} E$	$\Delta^{7''',8'''} E$
3	H	H	H	OMe	H	OH	$\Delta^{7'',8''} E$	$\Delta^{7''',8'''} E$
4	H	H	H	H	OMe	OH	$\Delta^{7'',8''} E$	$\Delta^{7''',8'''} E$
5	H	H	H	OMe	OMe	OH	$\Delta^{7'',8''} E$	$\Delta^{7''',8'''} E$
6	acetyl	H	H	H	H	OH	$\Delta^{7'',8''} E$	$\Delta^{7''',8'''} E$
7	H	acetyl	H	H	H	OH	$\Delta^{7'',8''} E$	$\Delta^{7''',8'''} E$
8	H	H	acetyl	H	H	OH	$\Delta^{7'',8''} E$	$\Delta^{7''',8'''} E$
9	acetyl	H	H	H	OMe	OH	$\Delta^{7'',8''} E$	$\Delta^{7''',8'''} E$
10	H	acetyl	H	H	OMe	OH	$\Delta^{7'',8''} E$	$\Delta^{7''',8'''} E$
11	H	H	acetyl	H	OMe	OH	$\Delta^{7'',8''} E$	$\Delta^{7''',8'''} E$
12	acetyl	H	H	OMe	H	OH	$\Delta^{7'',8''} E$	$\Delta^{7''',8'''} E$
13	H	acetyl	H	OMe	H	OH	$\Delta^{7'',8''} E$	$\Delta^{7''',8'''} E$
14	H	H	acetyl	OMe	H	OH	$\Delta^{7'',8''} E$	$\Delta^{7''',8'''} E$
15	acetyl	H	H	OMe	OMe	OH	$\Delta^{7'',8''} E$	$\Delta^{7''',8'''} E$
16	H	acetyl	H	OMe	OMe	OH	$\Delta^{7'',8''} E$	$\Delta^{7''',8'''} E$
17	H	H	acetyl	OMe	OMe	OH	$\Delta^{7'',8''} E$	$\Delta^{7''',8'''} E$
18	H	H	acetyl	OMe	OMe	OH	$\Delta^{7'',8''} Z$	$\Delta^{7''',8'''} E$
19	H	H	acetyl	OMe	OMe	OH	$\Delta^{7'',8''} E$	$\Delta^{7''',8'''} Z$
20	acetyl	acetyl	H	H	H	OH	$\Delta^{7'',8''} E$	$\Delta^{7''',8'''} E$
21	H	acetyl	acetyl	H	H	OH	$\Delta^{7'',8''} E$	$\Delta^{7''',8'''} E$
22	H	acetyl	acetyl	OMe	H	OH	$\Delta^{7'',8''} E$	$\Delta^{7''',8'''} E$
23	acetyl	acetyl	H	H	OMe	OH	$\Delta^{7'',8''} E$	$\Delta^{7''',8'''} E$
24	H	acetyl	acetyl	OMe	OMe	OH	$\Delta^{7'',8''} E$	$\Delta^{7''',8'''} E$

Figure 1. Chemical structures of compounds 1–24.

Table 1. ^1H NMR data of compounds 1–5 in δ ppm (J coupling in Hertz).

Position	1 ^a	2 ^b	3 ^a	4 ^a	5 ^a
1	3.51, d (12.0)	3.51, d (12.0)	3.52, d (12.0)	3.51, d (12.0)	3.51, d (11.6)
	3.31, d (12.0)	3.31, overlapped	3.32, d (12.0)	3.30, d (12.0)	3.31, overlapped
3	4.22, d (8.8)	4.22, d (9.0)	4.22, d (8.8)	4.22, d (8.4)	4.22, d (8.8)
4	4.04, t (8.8)	4.04, t (9.0)	4.04, t (8.8)	4.07, dd (9.2, 8.4)	4.07, t (8.8)
5	3.79, m	3.78, m	3.79, m	3.79, m	3.79, m
6	3.88, dd (12.0, 7.2)	3.88, dd (12.0, 7.2)	3.88, m	3.88, m	3.89, overlapped
	3.77, m	3.77, dd (12.0, 2.4)	3.77, m	3.77, m	3.78, m
1'	5.60, d (3.6)	5.60, d (3.6)	5.60, d (4.0)	5.60, d (3.6)	5.61, d (3.6)
2'	4.73, dd (10.0, 3.6)	4.73, dd (9.6, 3.6)	4.73, dd (10.0, 4.0)	4.73, dd (9.6, 3.6)	4.73, dd (9.6, 3.6)
3'	4.01, dd (10.0, 9.2)	4.01, t (9.6)	4.01, t (10.0)	4.01, t (9.6)	4.01, t (9.6)
4'	3.45, t (9.2)	3.46, t (9.6)	3.46, t (10.0)	3.45, t (9.6)	3.45, t (9.6)
5'	4.19, ddd (9.2, 6.0, 2.0)	4.20, m	4.18, dd (10.0, 6.0, 2.0)	4.20, m	4.20, m
	4.54, dd (12.0, 2.0)	4.56, br d (12.0)	4.54, dd (12.0, 2.0)	4.54, d (12.0)	4.54, br d (12.0)
6'	4.31, dd (12.0, 6.0)	4.34, dd (12.0, 6.6)	4.31, dd (12.0, 6.0)	4.31, dd (12.0, 6.4)	4.31, dd (12.0, 6.4)
2''	7.49, d (8.8)	7.49, d (8.4)	7.21, d (2.0)	7.48, d (8.4)	7.21, br s
3''	6.82, d (8.8)	6.81, d (8.4)		6.81, d (8.4)	
5''	6.82, d (8.8)	6.81, d (8.4)	6.82, d (8.0)	6.81, d (8.4)	6.82, d (8.4)
6''	7.49, d (8.8)	7.49, d (8.4)	7.11, dd (8.0, 2.0)	7.48, d (8.4)	7.11, br d (8.4)
7''	7.72, d (16.0)	7.72, d (16.2)	7.72, d (16.0)	7.72, d (16.0)	7.72, d (16.0)
8''	6.39, d (16.0)	6.39, d (16.2)	6.42, d (16.0)	6.39, d (16.0)	6.42, d (16.0)
2'''	7.51, d (8.8)	7.65, m	7.50, d (8.4)	7.25, br s	7.25, br s
3'''	6.81, d (8.8)	7.41, overlapped	6.81, d (8.4)		
4'''		7.41, overlapped			
5'''	6.81, d (8.8)	7.41, overlapped	6.81, d (8.4)	6.81, d (8.4)	6.81, d (8.4)
6'''	7.51, d (8.8)	7.65, m	7.50, d (8.4)	7.10, br d (8.4)	7.11, br d (8.4)
7'''	7.67, d (16.0)	7.75, d (16.2)	7.67, d (16.0)	7.65, d (16.0)	7.66, d (16.0)
8'''	6.43, d (16.0)	6.64, d (16.2)	6.43, d (16.0)	6.46, d (16.0)	6.46, d (16.0)
3''-OMe			3.90, s		3.90, s
3'''-OMe				3.89, s	3.90, s

^a In MeOH- d_4 , ^1H NMR at 400 MHz. ^b In MeOH- d_4 , ^1H NMR at 600 MHz. s = singlet; d = doublet; t = triplet; m = multiplet; br = broad.

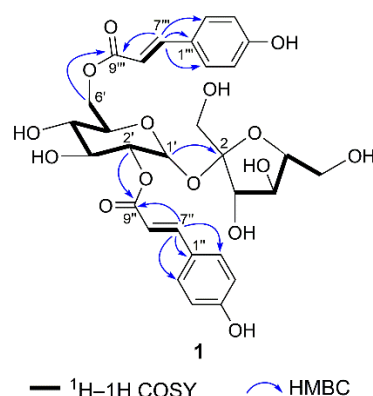
Table 2. ^{13}C NMR data of compounds 1–5 in δ ppm.

Position	1 ^a	2 ^b	3 ^a	4 ^a	5 ^a
1	62.9	62.9	62.9	62.9	63.0
2	105.7	105.7	105.7	105.6	105.7
3	77.0	77.0	77.0	77.0	77.0
4	75.6	75.6	75.6	75.7	75.7
5	84.0	84.0	84.0	84.0	84.0
6	64.2	64.2	64.2	64.2	64.2
1'	90.6	90.6	90.6	90.5	90.5
2'	74.4	74.4	74.4	74.4	74.4
3'	71.9	71.9	71.9	72.0	72.0
4'	72.0	72.0	72.0	72.0	72.0
5'	71.9	71.9	71.9	71.9	71.9
6'	65.0	65.2	65.0	65.0	65.1
1''	127.1	127.0	127.6	127.0	127.7
2''	131.3	131.3	111.8	131.3	111.8
3''	116.9	116.9	149.4	116.9	149.4
4''	161.6	161.7	151.0	161.6	151.0
5''	116.9	116.9	116.5	116.9	116.5
6''	131.3	131.3	124.3	131.3	124.3
7''	147.5	147.5	147.8	147.5	147.8
8''	114.7	114.7	114.9	114.7	115.0
9''	168.8	168.8	168.8	168.8	168.8
1'''	127.0	135.8	127.1	127.7	127.6

Table 2. Cont.

Position	1 ^a	2 ^b	3 ^a	4 ^a	5 ^a
2'''	131.3	129.4	131.3	111.6	111.6
3'''	116.8	130.0	116.8	149.4	149.4
4'''	161.4	131.6	161.4	150.7	150.8
5'''	116.8	130.0	116.8	116.4	116.4
6'''	131.3	129.4	131.3	124.3	124.3
7'''	146.9	146.7	146.9	147.1	147.1
8'''	114.9	118.7	115.0	115.2	115.2
9'''	169.2	168.5	169.2	169.1	169.1
3''-OMe			56.4		56.5
3'''-OMe				56.5	56.5

^a In MeOH-*d*₄, ¹³C NMR at 100 MHz. ^b In MeOH-*d*₄, ¹³C NMR at 150 MHz.

Figure 2. Key ¹H-¹H COSY and HMBC correlations of 1.

Compounds 2–24 were determined to be structurally related to 1 according to their extremely similar physicochemical properties and NMR data. The latter all showed the characteristics of a core D-sucrose unit, while the variation of substituents and their positions obtained different structures. The structural elucidation of 2–24 was as follows.

The molecular formula of compound 2 was assigned as C₃₀H₃₄O₁₄ based on its HRES-IMS (*m/z* 641.1847 [M + Na]⁺, calcd for 641.1841) and ¹³C NMR data, with 16 mass units less than 1. The analogous ¹H NMR data (Table 1) of 1 and 2 indicated that they were structural analogues, excepting of the presence of a monosubstituted aromatic moiety [δ_H 7.65 (1H, m, H-2'''/6'''), 7.41 (3H, overlapped, H-3'''/4'''/5''')] and the absence of an AA'BB' aromatic unit in 2. The long-range correlations from phenyl protons to olefinic carbons and correlations from olefinic protons to ester carbonyl carbons in the HMBC spectrum indicated that a *trans*-*p*-coumaroyl group and a *trans*-cinnamoyl group were presented (Figure 3). The HMBC correlations from H-2' (δ_H 4.73) to C-9'' and H₂-6' (δ_H 4.56, 4.34) to C-9''' confirmed the structure of 2 as shown, and this compound was named phaneroside B.

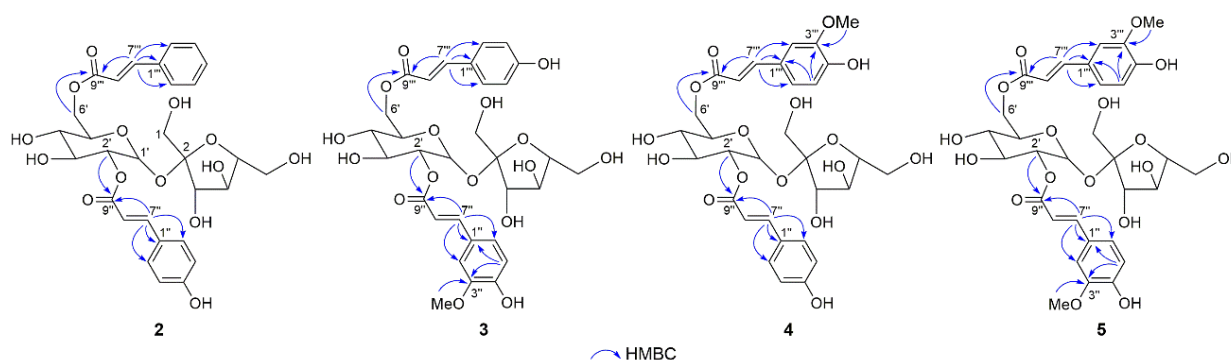


Figure 3. Key HMBC correlations of 2–5.

Compounds **3** and **4** had the same molecular formula, $C_{31}H_{36}O_{16}$, as determined using the HRESIMS peaks at m/z 687.1895 and 687.1896 ($[M + Na]^+$, calcd for 687.1896), respectively, indicating 30 mass units more than **1**, ascribed to a methoxy group. The 1H NMR data (Table 1) of **3** and **4** were similar to those of **1**, except for the presence of an ABX aromatic moiety [δ_H 7.21 (1H, d, $J = 2.0$ Hz, H-2''), 7.11 (1H, dd, $J = 8.0, 2.0$ Hz, H-6''), 6.82 (1H, d, $J = 8.0$ Hz, H-5'') in **3** and 7.25 (1H, br s, H-2'''), 7.10 (1H, br d, $J = 8.4$ Hz, H-6'''), 6.81 (1H, d, $J = 8.4$ Hz, H-5''') in **4**] and a methoxy [δ_H 3.90 (3H, s) in **3** and 3.89 (3H, s) in **4**] and the absence of an AA'BB' aromatic unit. The HMBC correlations from H-5''/3''-OMe to C-3'' in **3** and from H-5'''/3'''-OMe to C-3''' in **4**, together with the 1H - 1H COSY and HMBC correlations as mentioned previously, suggested that there were a *trans*-feruloyl group and a *trans*-*p*-coumaroyl group in both **3** and **4** (Figure 3). The complete structures of **3** and **4** were further established by the HMBC correlations from the protons of the sucrose unit to carbonyl carbons. Therefore, compounds **3** and **4** were determined to be phanerosides C and D, respectively.

Compound **5** gave the molecular formula of $C_{32}H_{38}O_{17}$, as determined by an HRESIMS ion at m/z 717.1990 ($[M + Na]^+$, calcd for 717.2001). The NMR data (Tables 1 and 2) indicated the presence of two *trans*-feruloyl moieties and a D-sucrose unit. The key HMBC cross-peaks from H-2' (δ_H 4.73) to C-9'' and H₂-6' (δ_H 4.54, 4.31) to C-9''' suggested that the two *trans*-feruloyl moieties were linked to C-2' and C-6' of glucopyranose unit (Figure 3). Thus, the structure of compound **5** was identified and named phaneroside E.

Compounds **6–8** shared the same molecular formula of $C_{32}H_{36}O_{16}$, as obtained from their respective HRESIMS data. Their molecular masses were 42 mass units more than that of **1**, which combined with the 1D NMR data of **6–8** (Tables 3 and 5) suggested that an acetyl group [δ_H 2.01 (3H, s), δ_C 172.0, 20.6 in **6**; δ_H 2.18 (3H, s), δ_C 172.2, 20.8 in **7**; δ_H 2.05 (3H, s), δ_C 172.4, 20.8 in **8**] existed in each compound. The key HMBC correlations from H₂-1 (δ_H 4.11, 4.06) to carbonyl (δ_C 172.0) in **6**, from H-3 (δ_H 5.43) to carbonyl (δ_C 172.2) in **7**, and from H-4 (δ_H 5.30) to carbonyl (δ_C 172.4) in **8** indicated that the acetyl group was attached to C-1, C-3, and C-4 of the fructofuranose unit in compounds **6**, **7**, and **8**, respectively (Figure 4). In addition, the chemical shifts of the protons linked to the acetyl group in **6–8** were obviously shifted downfield compared to those of **1**, which also supported the above description. Thus, the structures of **6**, **7**, and **8** were established and named phanerosides F, G, and H, respectively.

Table 3. 1H NMR data (400 MHz) of compounds **6–11** in MeOH- d_4 .

Position	6	7	8	9	10	11
1	4.11, d (11.6)	3.54, d (12.0)	3.57, d (12.0)	4.11, d (12.0)	3.54, d (12.0)	3.57, br d (12.0)
3	4.06, d (11.6)	3.35, d (12.0)	3.40, d (12.0)	4.06, d (12.0)	3.34, d (12.0)	3.40, br d (12.0)
4	4.08, d (8.8)	5.43, d (8.4)	4.47, d (8.4)	4.08, d (6.8)	5.44, d (8.4)	4.47, d (8.4)
5	4.04, t (8.8)	4.35, t (8.4)	5.30, t (8.4)	4.07, t (6.8)	4.39, t (8.4)	5.28, dd (8.4, 7.6)
6	3.79, m	3.90, m	3.91, m	3.79, m	3.91, m	3.91, overlapped
1-OAc	3.88, dd (11.6, 7.2)	3.84, dd (12.0, 6.4)	3.92, m	3.89, overlapped	3.85, dd (11.6, 6.8)	3.93, m
3-OAc	3.75, m	3.78, dd (12.0, 3.2)	3.77, dd (11.2, 2.4)	3.76, m	3.78, dd (11.6, 2.8)	3.80, dd (11.2, 2.8)
4-OAc	2.01, s	2.18, s	2.05, s	2.01, s	2.18, s	2.04, s
1'	5.65, d (3.6)	5.63, d (3.6)	5.65, d (3.6)	5.66, d (3.6)	5.63, d (3.6)	5.65, d (3.6)
2'	4.79, dd (10.4, 3.6)	4.72, dd (10.0, 3.6)	4.76, dd (10.0, 3.6)	4.80, dd (10.0, 3.6)	4.73, dd (10.4, 3.6)	4.76, dd (10.0, 3.6)
3'	4.00, dd (10.4, 9.2)	3.88, t (10.0)	4.01, dd (10.0, 9.6)	4.00, dd (10.0, 8.8)	3.88, overlapped	4.01, t (10.0)
4'	3.46, dd (10.0, 9.2)	3.47, t (10.0)	3.43, t (9.6)	3.45, dd (10.0, 8.8)	3.45, dd (10.0, 8.8)	3.44, t (10.0)
5'	4.20, ddd (10.0, 6.0, 2.0)	4.16, ddd (10.0, 6.0, 2.0)	4.23, m	4.21, ddd (10.0, 6.8, 2.0)	4.19, ddd (10.0, 6.8, 2.0)	4.24, ddd (10.0, 6.4, 1.6)
6'	4.54, dd (12.0, 2.0)	4.56, dd (12.0, 2.0)	4.57, dd (12.0, 1.6)	4.54, dd (12.0, 2.0)	4.56, dd (12.0, 2.0)	4.57, dd (12.0, 1.6)
2''	4.31, dd (12.0, 6.0)	4.32, dd (12.0, 6.0)	4.31, dd (12.0, 6.4)	4.30, dd (12.0, 6.8)	4.31, dd (12.0, 6.8)	4.32, dd (12.0, 6.4)
3''	7.49, d (8.8)	7.48, d (8.8)	7.49, d (8.4)	7.49, d (8.8)	7.48, d (8.8)	7.49, d (8.8)
5''	6.80, d (8.8)	6.82, d (8.8)	6.81, d (8.4)	6.81, d (8.8)	6.81, d (8.8)	6.81, d (8.8)
6''	6.80, d (8.8)	6.82, d (8.8)	6.81, d (8.4)	6.81, d (8.8)	6.81, d (8.8)	6.81, d (8.8)
7''	7.49, d (8.8)	7.48, d (8.8)	7.49, d (8.4)	7.49, d (8.8)	7.48, d (8.8)	7.49, d (8.8)
8''	7.71, d (16.0)	7.70, d (16.0)	7.70, d (16.0)	7.71, d (16.0)	7.69, d (16.0)	7.70, d (16.0)
2'''	6.39, d (16.0)	6.37, d (16.0)	6.40, d (16.0)	6.41, d (16.0)	6.37, d (16.0)	6.41, d (16.0)
3'''	7.50, d (8.8)	7.51, d (8.8)	7.51, d (8.4)	7.26, d (2.0)	7.25, d (2.0)	7.25, d (2.0)
5'''	6.80, d (8.8)	6.80, d (8.8)	6.80, d (8.4)	6.81, d (8.0)	6.81, d (8.0)	6.81, d (8.4)
6'''	6.80, d (8.8)	6.80, d (8.8)	6.80, d (8.4)	6.81, d (8.0)	6.81, d (8.0)	6.81, d (8.4)
7'''	7.50, d (8.8)	7.50, d (8.8)	7.51, d (8.4)	7.11, dd (8.0, 2.0)	7.09, dd (8.0, 2.0)	7.11, dd (8.4, 2.0)
8'''	7.66, d (16.0)	7.66, d (16.0)	7.65, d (16.0)	7.65, d (15.6)	7.65, d (16.0)	7.65, d (16.0)
3''-OMe	6.43, d (16.0)	6.43, d (16.0)	6.49, d (16.0)	6.47, d (15.6)	6.47, d (16.0)	6.52, d (16.0)
3'''-OMe				3.90, s	3.89, s	3.90, s

s = singlet; d = doublet; t = triplet; m = multiplet; br = broad.

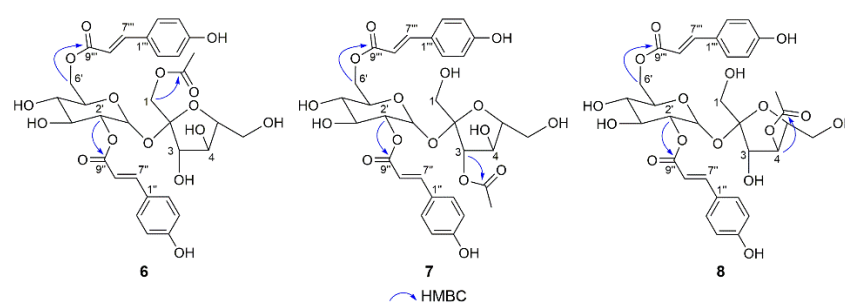


Figure 4. Key HMBC correlations of **6**, **7**, and **8**.

Compounds **9–11** were assigned the same molecular formula, $C_{33}H_{38}O_{17}$, according to their HRESIMS and ^{13}C NMR data. Compounds **9–11** were determined to be acetylated derivatives of **4**, as their molecular masses were 42 mass units more than that of **4**. Their 1H and ^{13}C NMR data (Tables 3 and 5) showed the characteristics of the acetyl group [δ_H 2.01 (3H, s), δ_C 172.0, 20.6 in **9**; δ_H 2.18 (3H, s), δ_C 172.2, 20.8 in **10**; δ_H 2.04 (3H, s), δ_C 172.4, 20.8 in **11**]. Furthermore, the key HMBC correlations from H₂-1 (δ_H 4.11, 4.06) to carbonyl (δ_C 172.0) in **9**, from H-3 (δ_H 5.44) to carbonyl (δ_C 172.2) in **10**, and from H-4 (δ_H 5.28) to carbonyl (δ_C 172.4) in **11** located the acetyl group at C-1, C-3, and C-4 for compounds **9**, **10**, and **11**, respectively. Thus, the structures of compounds **9–11** (phanerosides I–K) were defined as shown.

Compounds **12–14** possessed identical molecular formula, $C_{33}H_{38}O_{17}$, as determined by their respective HRESIMS ion peaks at m/z 729.2018, 729.2010, and 729.1990 ($[M + Na]^+$, calcd for 729.2001), which were 42 mass units more than that of **3**. Detailed analysis of their 1D NMR data (Tables 4 and 5) indicated that compounds **12–14** were acetylated derivatives of **3**, with a difference in the position of the acetyl group. In their HMBC spectra, the correlations from H₂-1 (δ_H 4.14, 4.03) to carbonyl (δ_C 172.0) in **12**, from H-3 (δ_H 5.43) to carbonyl (δ_C 172.2) in **13**, and from H-4 (δ_H 5.31) to carbonyl (δ_C 172.3) in **14** suggested that the acetyl group was linked to C-1, C-3, and C-4 in **12**, **13**, and **14**, respectively. Therefore, the structures of compounds **12–14** (phanerosides L–N) were established as shown.

Compounds **15–17** were determined to have the same molecular formula, $C_{34}H_{40}O_{18}$, on the basis of their HRESIMS and ^{13}C NMR data, displaying 42 mass units more than that of **5**. Compounds **15–17** were suggested to be acetylated derivatives of **5** after an analysis of their 1D NMR data (Tables 4 and 5). The acetyl group was, respectively, located at C-1, C-3, and C-4 of the fructofuranose unit in **15**, **16**, and **17**, which was confirmed using the key HMBC correlations from the protons of the sugar unit to corresponding carbonyl carbons. Accordingly, the structure of compounds **15–17** (phanerosides O–Q) were determined as shown.

Compounds **18** and **19** had the same molecular formula, $C_{34}H_{40}O_{18}$, as **17** according to their HRESIMS and ^{13}C NMR data. The 1D NMR data (Tables 4 and 5) closely resembled those of **17**, with the exception that one of the two *trans*-feruloyl groups was replaced by a *cis*-feruloyl group according to the smaller coupling constants of $^3J_{7'',8''}$ (12.6 Hz) in **18** and $^3J_{7''',8'''}$ (13.2 Hz) in **19**. The *cis*-feruloyl group was linked to C-2' and C-6' of the glucopyranose unit in **18** and **19**, respectively, which was proved by the key HMBC cross-peaks from H-2'/H-7'' to C-9'' in **18** and from H-6'/H-7''' to C-9''' in **19** (Figure 5). Thus, the structures of compounds **18** and **19** were identified and named phanerosides R and S, respectively.

Table 4. ¹H NMR data of compounds 12–19.

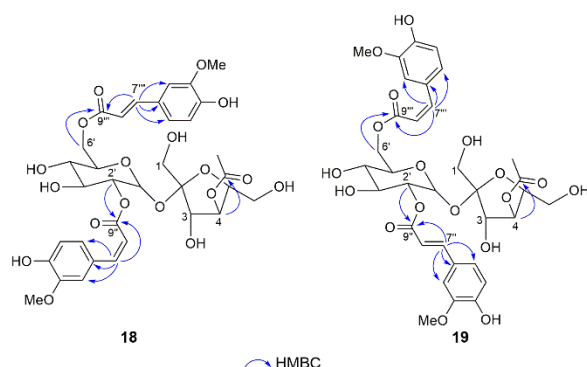
Position	12 ^a	13 ^a	14 ^a	15 ^a	16 ^b	17 ^a	18 ^b	19 ^b
1	4.14, d (12.4)	3.55, d (11.6)	3.59, d (12.0)	4.14, d (11.6)	3.54, d (12.0)	3.59, d (12.0)	3.55, d (12.0)	3.58, d (12.0)
	4.03, d (12.4)	3.36, d (11.6)	3.42, d (12.0)	4.02, d (11.6)	3.34, d (12.0)	3.42, d (12.0)	3.39, d (12.0)	3.42, d (12.0)
3	4.09, d (8.4)	5.43, d (8.4)	4.47, d (8.0)	4.09, d (8.4)	5.44, d (8.4)	4.48, d (8.8)	4.47, d (8.4)	4.46, d (8.4)
4	4.04, t (8.4)	4.35, t (8.4)	5.31, t (8.0)	4.08, t (8.4)	4.39, t (8.4)	5.29, dd (8.8, 7.6)	5.26, t (8.4)	5.29, t (8.4)
5	3.79, m	3.90, overlapped	3.91, overlapped	3.80, m	3.91, overlapped	3.91, overlapped	3.90, overlapped	3.90, overlapped
	3.88, m	3.84, dd (12.0, 6.4)	3.92, overlapped	3.89, overlapped	3.85, dd (12.0, 6.6)	3.92, overlapped	3.92, overlapped	3.90, overlapped
6	3.75, dd (11.6, 2.8)	3.78, dd (12.0, 3.2)	3.78, m	3.76, dd (11.6, 2.8)	3.79, dd (12.0, 2.4)	3.81, dd (11.2, 2.4)	3.78, dd (10.8, 2.4)	3.78, m
1-OAc	2.02, s			2.02, s				
3-OAc		2.18, s			2.18, s			
4-OAc			2.04, s			2.03, s	2.08, s	2.05, s
1'	5.64, d (3.6)	5.63, d (4.0)	5.67, d (3.6)	5.65, d (4.0)	5.64, d (3.6)	5.66, d (4.0)	5.62, d (3.6)	5.66, d (3.6)
2'	4.82, dd (10.4, 3.6)	4.72, dd (10.4, 4.0)	4.76, dd (10.0, 3.6)	4.82, dd (10.0, 4.0)	4.72, dd (10.2, 3.6)	4.76, dd (10.0, 4.0)	4.75, dd (10.2, 3.6)	4.73, dd (10.2, 3.6)
3'	4.00, dd (10.4, 9.2)	3.88, overlapped	4.01, t (10.0)	4.00, dd (10.0, 8.8)	3.87, t (10.2)	4.01, dd (10.0, 8.8)	3.98, dd (10.2, 9.6)	3.99, dd (10.2, 9.0)
4'	3.46, dd (10.0, 9.2)	3.47, t (10.0)	3.43, t (10.0)	3.46, dd (10.0, 8.8)	3.45, t (10.2)	3.44, dd (10.0, 8.8)	3.43, t (9.6)	3.43, dd (10.2, 9.0)
5'	4.20, ddd (10.0, 6.4, 2.0)	4.16, ddd (10.0, 6.0, 2.0)	4.23, dd (10.0, 6.4)	4.22, ddd (10.0, 6.4, 2.0)	4.19, m	4.23, ddd (10.0, 6.4, 1.6)	4.23, ddd (9.6, 6.6, 1.8)	4.19, ddd (10.2, 5.4, 1.8)
	4.54, dd (12.0, 2.0)	4.56, dd (12.0, 2.0)	4.57, br d (12.0)	4.54, dd (12.0, 2.0)	4.56, br d (12.0)	4.57, dd (12.0, 1.6)	4.56, dd (12.0, 1.8)	4.53, dd (12.0, 1.8)
6'	4.31, dd (12.0, 6.4)	4.32, dd (12.0, 6.0)	4.31, dd (12.0, 6.4)	4.30, dd (12.0, 6.4)	4.31, dd (12.0, 6.6)	4.32, dd (12.0, 6.4)	4.31, dd (12.0, 6.6)	4.30, dd (12.0, 5.4)
2''	7.26, d (2.0)	7.21, d (2.0)	7.23, d (2.0)	7.26, d (2.4)	7.21, br s	7.23, d (2.0)	7.93, d (2.4)	7.23, d (1.8)
5''	6.81, d (8.4)	6.82, d (8.0)	6.82, d (8.0)	6.81, d (8.0)	6.82, d (7.8)	6.81, d (8.0)	6.77, d (8.4)	6.81, d (8.4)
6''	7.09, dd (8.4, 2.0)	7.10, dd (8.0, 2.0)	7.09, dd (8.0, 2.0)	7.09, dd (8.0, 2.4)	7.10, overlapped	7.09, dd (8.0, 2.0)	7.19, dd (8.4, 2.4)	7.09, dd (8.4, 1.8)
7''	7.70, d (15.6)	7.69, d (15.6)	7.69, d (16.0)	7.70, d (16.0)	7.69, d (16.2)	7.69, d (16.0)	6.92, d (12.6)	7.68, d (15.6)
8''	6.45, d (15.6)	6.39, d (15.6)	6.44, d (16.0)	6.45, d (16.0)	6.40, d (16.2)	6.44, d (16.0)	5.88, d (12.6)	6.44, d (15.6)
2'''	7.51, d (8.4)	7.50, d (8.8)	7.51, d (8.0)	7.26, d (2.4)	7.26, br s	7.24, d (2.0)	7.25, d (2.4)	7.87, d (1.8)
3'''	6.81, d (8.4)	6.80, d (8.8)	6.80, d (8.0)					
5'''	6.81, d (8.4)	6.80, d (8.8)	6.80, d (8.0)	6.81, d (8.0)	6.80, d (7.8)	6.81, d (8.0)	6.81, d (8.4)	6.77, d (8.4)
6'''	7.51, d (8.4)	7.50, d (8.8)	7.51, d (8.0)	7.11, dd (8.0, 2.4)	7.10, overlapped	7.11, dd (8.0, 2.0)	7.11, dd (8.4, 2.4)	7.15, dd (8.4, 1.8)
7'''	7.66, d (15.6)	7.66, d (15.6)	7.65, d (16.0)	7.65, d (16.0)	7.65, d (16.2)	7.65, d (16.0)	7.65, d (16.2)	6.88, d (13.2)
8'''	6.43, d (15.6)	6.43, d (15.6)	6.49, d (16.0)	6.47, d (16.0)	6.47, d (16.2)	6.52, d (16.0)	6.53, d (16.2)	5.90, d (13.2)
3''-OMe	3.92, s	3.90, s	3.92, s	3.92, s	3.90, s	3.92, s	3.88, s	3.92, s
3'''-OMe				3.90, s	3.89, s	3.90, s	3.90, s	3.89, s

^a In MeOH-*d*₄, ¹H NMR at 400 MHz. ^b In MeOH-*d*₄, ¹H NMR at 600 MHz. s = singlet; d = doublet; t = triplet; m = multiplet; br = broad.

Table 5. ^{13}C NMR data of compounds **12**–**19**.

Position	6 ^a	7 ^a	8 ^a	9 ^a	10 ^a	11 ^a	12 ^a	13 ^a	14 ^a	15 ^a	16 ^b	17 ^a	18 ^b	19 ^b
1	64.8	64.4	62.5	64.8	64.5	62.5	64.8	64.5	62.5	64.8	64.5	62.5	62.5	62.3
2	103.9	105.0	106.0	103.8	104.9	106.0	103.9	105.0	106.1	103.8	104.9	106.1	105.9	106.2
3	78.5	78.6	75.2	78.5	78.6	75.2	78.4	78.7	75.2	78.4	78.6	75.2	75.2	75.2
4	75.3	73.8	78.0	75.4	73.8	78.1	75.4	73.8	78.0	75.4	73.8	78.2	78.2	77.9
5	84.1	84.2	82.2	84.1	84.2	82.3	84.2	84.2	82.3	84.2	84.2	82.3	82.3	82.3
6	64.1	63.9	64.8	64.2	64.0	64.8	64.2	63.9	64.9	64.3	64.0	64.9	64.8	64.8
1-OAc	172.0			172.0			172.0			172.0				
	20.6			20.6			20.6			20.6				
3-OAc		172.2			172.2			172.2			172.2			
		20.8			20.8			20.8			20.8			
4-OAc			172.4			172.4			172.3			172.4	172.4	172.3
			20.8			20.8			20.8			20.8	20.9	20.8
1'	90.9	90.5	91.1	90.9	90.4	91.1	91.0	90.6	91.2	90.9	90.4	91.2	91.0	91.3
2'	74.1	74.3	74.2	74.1	74.3	74.3	74.1	74.3	74.2	74.1	74.3	74.2	73.9	74.2
3'	72.1	72.3	72.0	72.2	72.3	72.0	72.2	72.3	72.0	72.2	72.3	72.1	71.9	72.0
4'	72.0	71.8	72.0	72.0	71.9	72.1	72.1	72.0	72.1	72.0	71.9	72.0	72.1	71.9
5'	72.0	72.0	72.0	72.0	72.0	72.0	72.0	71.8	72.0	72.0	72.0	72.0	72.0	71.8
6'	65.0	64.9	65.1	65.1	65.1	65.1	65.0	64.9	65.1	65.1	65.1	65.1	65.1	64.5
1''	127.1	127.1	127.0	127.2	127.0	127.1	127.7	127.5	127.7	127.8	127.5	127.6	127.9	127.5
2''	131.3	131.3	131.3	131.4	131.3	131.4	111.7	111.8	111.7	111.6	111.8	111.8	115.3	111.7
3''	116.9	116.8	116.9	116.8	116.9	116.8	149.4	149.5	149.4	149.4	149.5	149.4	148.3	149.5
4''	161.7	161.6	161.6	161.4	161.6	161.4	150.8	151.5	150.8	150.8	151.1	150.9	149.9	150.9
5''	116.9	116.8	116.9	116.8	116.9	116.8	116.4	116.6	116.4	116.4	116.5	116.4	115.6	116.5
6''	131.3	131.3	131.3	131.4	131.3	131.4	124.5	124.3	124.4	124.5	124.3	124.4	127.4	124.5
7''	147.5	147.5	147.4	147.5	147.5	147.3	147.7	147.8	147.5	147.7	147.8	147.6	147.0	147.5
8''	114.8	114.6	114.9	114.9	114.6	114.9	115.2	114.9	115.2	115.2	114.9	115.2	115.8	115.1
9''	168.8	168.7	168.8	168.8	168.7	168.8	168.7	168.7	168.8	168.7	168.7	168.8	167.5	168.8
1'''	127.1	127.0	127.2	127.7	127.6	127.8	127.2	127.1	127.3	127.7	127.6	127.8	127.7	128.0
2'''	131.4	131.3	131.4	111.6	111.5	111.9	131.3	131.3	131.3	111.7	111.5	111.7	111.8	115.1
3'''	116.9	116.9	116.8	149.4	149.4	149.4	116.8	116.9	116.8	149.4	149.5	149.4	149.4	148.4
4'''	161.6	161.4	161.4	150.7	150.8	150.6	161.4	161.5	161.3	150.7	150.9	150.7	150.8	149.7
5'''	116.9	116.9	116.8	116.4	116.4	116.4	116.8	116.9	116.8	116.4	116.4	116.5	116.4	115.7
6'''	131.4	131.3	131.4	124.4	124.4	124.4	131.3	131.3	131.3	124.4	124.5	124.4	124.4	127.0
7'''	146.9	146.9	146.8	147.1	147.1	147.1	146.9	146.9	146.8	147.1	147.2	147.1	147.1	146.0
8'''	114.9	114.9	115.2	115.3	115.2	115.4	115.0	114.9	115.3	115.3	115.2	115.4	115.4	116.1
9'''	169.2	169.2	169.3	169.1	169.1	169.3	169.2	169.2	169.3	169.1	169.1	169.3	169.3	168.1
3''-OMe						56.5	56.5	56.4	56.5	56.5	56.5	56.5	56.4	56.4
3'''-OMe				56.5	56.5					56.5	56.4	56.5	56.5	56.4

^a In MeOH- d_4 , ^{13}C NMR at 100 MHz. ^b In MeOH- d_4 , ^{13}C NMR at 150 MHz.

**Figure 5.** Key HMBC correlations of **18** and **19**.

Compounds **20** and **21** were suggested to have the same molecular formula, $\text{C}_{34}\text{H}_{38}\text{O}_{17}$, owing to their coincident positive HRESIMS ion at m/z 741.2001 [$\text{M} + \text{Na}$]⁺ (calcd for 741.2001), indicating 42 mass units more than that of **7**. Comparison of their 1D NMR data (Tables 6 and 7) with those of **7** disclosed that one more acetyl group was presented in both **20** and **21**. The key HMBC correlations from H₂-1 (δ_{H} 4.17, 4.00) to carbonyl (δ_{C} 172.0) and H-3 (δ_{H} 5.29) to carbonyl (δ_{C} 172.1) in **20**, and from H-3 (δ_{H} 5.65) to carbonyl (δ_{C} 171.8) and H-4 (δ_{H} 5.48) to carbonyl (δ_{C} 172.0) in **21**, indicated that the two acetyl groups were located

at C-1 and C-3 in **20** and C-3 and C-4 in **21** (Figure 6). Thus, the structures of compounds **20** and **21** were characterized and named phanerosides T and U, respectively.

Table 6. ^1H NMR data of compounds **20–24**.

Position	20 ^a	21 ^a	22 ^b	23 ^a	24 ^a
1	4.17, d (12.0)	3.57, d (12.0)	3.58, d (12.0)	4.16, d (11.6)	3.59, d (12.0)
	4.00, d (12.0)	3.45, d (12.0)	3.47, d (12.0)	3.99, d (11.6)	3.48, d (12.0)
3	5.29, d (8.0)	5.65, d (7.6)	5.65, d (7.8)	5.30, d (8.4)	5.65, d (7.6)
4	4.34, t (8.0)	5.48, t (7.6)	5.50, t (7.8)	4.38, t (8.4)	5.49, t (7.6)
5	3.89, m	4.07, m	4.08, m	3.90, overlapped	4.08, td (7.6, 4.4)
6	3.84, dd (11.6, 6.8)	3.87, dd (12.0, 6.8)	3.87, dd (12.0, 7.2)	3.85, dd (12.0, 6.8)	3.87, overlapped
	3.77, dd, (11.6, 2.8)	3.77, dd (12.0, 4.4)	3.78, dd (12.0, 4.2)	3.77, dd (12.0, 2.8)	3.80, dd (12.0, 4.4)
1-OAc	2.02, s			2.02, s	
3-OAc	2.17, s	2.11, s	1.98, s	2.18, s	2.11, s
4-OAc		1.99, s	2.10, s		1.97, s
1'	5.66, d (3.6)	5.62, d (3.6)	5.62, d (3.6)	5.66, d (3.6)	5.62, d (3.6)
2'	4.78, dd (10.0, 3.6)	4.76, dd (10.0, 3.6)	4.77, dd (10.2, 3.6)	4.78, dd (10.0, 3.6)	4.77, dd (10.0, 3.6)
3'	3.88, dd (10.0, 9.2)	3.91, dd (10.0, 9.2)	3.91, m	3.88, m	3.91, overlapped
4'	3.47, t (9.2)	3.47, t (9.2)	3.46, t (10.2)	3.46, dd (10.0, 9.2)	3.47, m
5'	4.16, m	4.19, ddd (10.0, 6.0, 2.0)	4.18, ddd (10.2, 6.0, 1.8)	4.18, m	4.19, ddd (10.0, 6.4, 2.0)
6'	4.57, dd (12.0, 2.0)	4.60, dd (12.0, 2.0)	4.59, dd (12.0, 1.8)	4.57, dd (12.0, 2.0)	4.60, dd (12.0, 2.0)
	4.32, dd (12.0, 6.0)	4.33, dd (12.0, 6.0)	4.32, dd (12.0, 6.0)	4.30, dd (12.0, 6.8)	4.33, dd (12.0, 6.4)
2''	7.49, d (8.8)	7.49, d (8.8)	7.25, br s	7.49, d (8.8)	7.24, d (2.0)
3''	6.81, d (8.8)	6.81, d (8.8)		6.81, d (8.8)	
5''	6.81, d (8.8)	6.81, d (8.8)	6.81, d (8.4)	6.81, d (8.8)	6.82, d (8.0)
6''	7.49, d (8.8)	7.49, d (8.8)	7.10, dd (8.4, 1.8)	7.49, d (8.8)	7.10, dd (8.0, 2.0)
7''	7.68, d (15.6)	7.69, d (16.0)	7.69, d (16.2)	7.68, d (16.0)	7.69, d (16.0)
8''	6.38, d (15.6)	6.41, d (16.0)	6.45, d (16.2)	6.38, d (16.0)	6.45, d (16.0)
2'''	7.50, d (8.8)	7.50, d (8.8)	7.49, d (8.4)	7.26, d (2.0)	7.24, d (2.0)
3'''	6.81, d (8.8)	6.81, d (8.8)	6.80, d (8.4)		
5'''	6.81, d (8.8)	6.81, d (8.8)	6.80, d (8.4)	6.81, d (8.0)	6.82, d (8.0)
6'''	7.50, d (8.8)	7.50, d (8.8)	7.49, d (8.4)	7.09, dd (8.0, 2.0)	7.10, dd (8.0, 2.0)
7'''	7.66, d (16.0)	7.65, d (16.0)	7.65, d (16.2)	7.65, d (16.0)	7.65, d (16.0)
8'''	6.43, d (16.0)	6.45, d (16.0)	6.44, d (16.2)	6.47, d (16.0)	6.49, d (16.0)
3''-OMe			3.91, s		3.90, s
3'''-OMe				3.89, s	3.91, s

^a In MeOH- d_4 , ^1H NMR at 400 MHz. ^b In MeOH- d_4 , ^1H NMR at 600 MHz. s = singlet; d = doublet; t = triplet; m = multiplet; br = broad.

Table 7. ^{13}C NMR data of compounds **20–24**.

Position	20 ^a	21 ^a	22 ^b	23 ^a	24 ^a
1	66.1	63.6	63.4	66.2	63.5
2	103.3	106.1	106.2	103.2	106.2
3	79.5	76.6	76.6	79.5	76.7
4	73.5	76.5	76.5	73.5	76.6
5	84.2	82.7	82.7	84.3	82.7
6	63.8	64.1	64.2	63.9	64.3
1-OAc	172.0			171.9	
	20.6			20.6	
3-OAc	172.1	171.8	172.0	172.1	171.7
	20.7	20.7	20.7	20.7	20.7
4-OAc		172.0	171.8		172.0
		20.7	20.7		20.7
1'	91.0	91.3	91.4	90.9	91.4
2'	74.0	74.1	74.1	74.0	74.1
3'	72.3	72.2	72.2	72.4	72.2
4'	71.8	71.8	71.9	71.9	71.9
5'	72.2	72.2	72.2	72.2	72.2

Table 7. Cont.

Position	20 ^a	21 ^a	22 ^b	23 ^a	24 ^a
6'	64.9	64.9	64.9	65.1	64.9
1''	127.1	127.2	127.4	127.1	127.6
2''	131.3	131.3	111.7	131.4	111.7
3''	116.8	116.8	149.5	116.8	149.4
4''	161.5	161.6	151.2	161.5	150.7
5''	116.8	116.8	116.5	116.8	116.4
6''	131.3	131.3	124.6	131.4	124.3
7''	147.5	147.5	147.8	147.5	147.8
8''	114.7	114.8	115.0	114.8	115.1
9''	168.7	168.7	168.7	168.7	168.7
1'''	127.1	127.0	127.1	127.7	127.8
2'''	131.4	131.4	131.3	111.5	111.8
3'''	116.8	116.9	116.9	149.4	149.4
4'''	161.4	161.4	161.6	150.7	150.8
5'''	116.8	116.9	116.9	116.4	116.4
6'''	131.4	131.4	131.3	124.5	124.5
7'''	146.9	146.8	146.9	147.1	147.1
8'''	114.9	115.1	115.0	115.3	115.4
9'''	169.2	169.2	169.2	169.1	169.2
3''-OMe			56.4		56.5
3'''-OMe				56.5	56.5

^a In MeOH-*d*₄, ¹³C NMR at 100 MHz. ^b In MeOH-*d*₄, ¹³C NMR at 150 MHz.

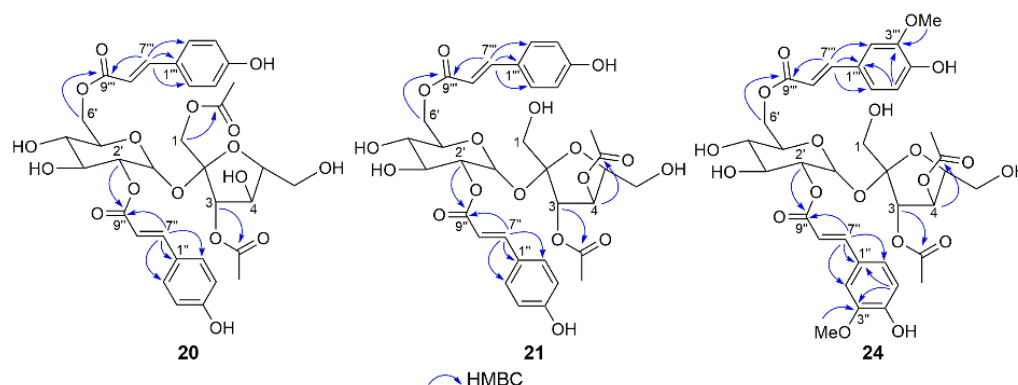


Figure 6. Key HMBC correlations of 20, 21, and 24.

Compounds **22** and **23** showed the same molecular formula, C₃₅H₄₀O₁₈, as determined by their ¹³C NMR data and respective HRESIMS ion peaks at *m/z* 771.2093 and 771.2112 ([M + Na]⁺, calcd for 771.2107). Analysis of the NMR data (Figures S194–S199 and S203–S208) of **22** and **23** proclaimed that the sugar moieties in both compounds were acylated by a *trans*-ferulic acid, a *trans*-*p*-coumaric acid, and two acetic acids. The *trans*-feruloyl and *trans*-*p*-coumaroyl units were, respectively, located at C-2' and C-6' in **22** based on the key HMBC correlations from H-2' to C-9'' and H₂-6' to C-9''', while the locations of these two substituents in **23** were the opposite. The key HMBC correlations from H-3 (δ_H 5.65) to carbonyl (δ_C 172.0) and H-4 (δ_H 5.50) to carbonyl (δ_C 171.8) in **22**, and from H₂-1 (δ_H 4.16, 3.99) to carbonyl (δ_C 171.9) and H-3 (δ_H 5.30) to carbonyl (δ_C 172.1) in **23**, indicated that the two acetyl groups were placed at C-3 and C-4 in **22** and C-1 and C-3 in **23**. Accordingly, the structures of compounds **22** and **23** (phanerosides V and W) were defined as shown.

The molecular formula of compound **24** was assigned as C₃₆H₄₂O₁₉ based on the HRESIMS (*m/z* 801.2226 [M + Na]⁺, calcd for 801.2213) and ¹³C NMR data. The NMR data (Figures S212–S217) indicated that it possessed two *trans*-feruloyl moieties, D-sucrose, and two acetyl groups. The two *trans*-feruloyl moieties were linked to C-2' and C-6' of the glucopyranose ring, and two acetyl groups were attached to C-3 and C-4 of the

fructofuranose ring, according to the key HMBC correlations as shown in Figure 6. Thus, the structure of compound **24** was identified and named phaneroside X.

a. In Vitro Anti-inflammatory Effects of Compounds 1–24

Nitric oxide (NO) is one of the major inflammatory mediators, and phenylpropanoid esters of sucrose have been previously reported to possess potent anti-inflammatory activity [3,7,22]. Therefore, all the isolates were evaluated in vitro for their anti-inflammatory potential via the Griess reaction in LPS-induced BV-2 microglial cells (Figure 7) [23]. Especially, compounds **6** and **21** exhibited potent inhibitory activities on NO production, with IC_{50} values of 6.7 ± 1.7 and 5.2 ± 3.5 μ M, which were better than the positive control, L-NMMA ($IC_{50} = 7.0 \pm 2.7$ μ M). Compounds **10**, **14**, and **19** showed moderate inhibitory effects on NO production, with IC_{50} values of 72.7, 46.0, and 57.7 μ M, respectively. These results suggested that the anti-inflammatory activities of these compounds were not determined by a single variable, while the type, number, and position of the substituents may all affect their inhibitory activities.

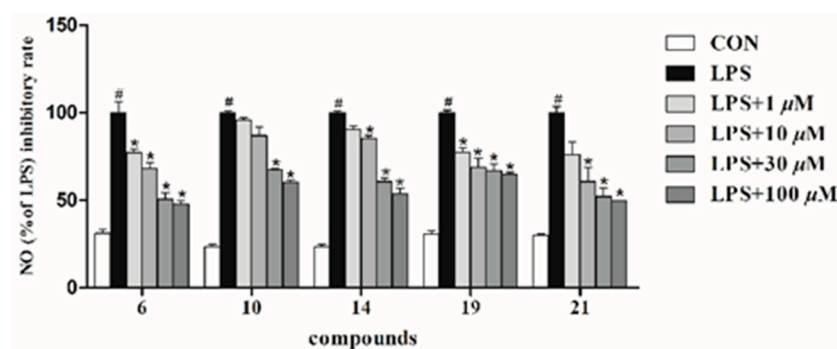


Figure 7. Effects of compounds **6**, **10**, **14**, **19**, and **21** on NO inhibitory activity (1–100 μ M) in BV-2 microglial cells. * $p < 0.001$, compared with the LPS-treated group; # $p < 0.001$, compared with the control group.

b. Antioxidant Effects of Compounds 1–24

Many isolated phenylpropanoid esters of sucrose are thought to act as potential antioxidants [3]. Consequently, their antioxidant activities were also tested using the DPPH radical scavenging assay [24]. Compounds **5**, **15**, **17**, and **24** exhibited moderate inhibitory effects with EC_{50} values of 43.9 ± 0.2 , 43.8 ± 0.1 , 34.9 ± 0.1 , 39.4 ± 0.3 μ M, respectively. As it stands, the compounds whose C-2' and C-6' of the glucopyranose ring were both substituted by *trans*-feruloyl groups showed a more positive impact on their antioxidant effects.

3. Materials and Methods

General Experimental Procedures

Optical rotations were obtained on a JASCO P-2000 polarimeter. UV absorption spectra were determined on a PerkinElmer 650 spectrophotometer. NMR spectra were acquired on a 400 or 600 MHz Bruker AVANCE apparatus. Chemical shifts are expressed in δ (ppm) and referenced to the solvent residual peak. HRESIMS data were obtained on an Agilent 6545 Q-TOF LC-MS spectrometer. The other instruments and materials serving for the isolation and purification of compounds were coincident with previous papers [25,26].

a. Plant Material

The rattans of *P. championii* Benth. were collected in November 2020 in Guilin, Guangxi Province, People's Republic of China (GPS: 24°47'32.7" N 110°27'36.8" E). The specimen (No. PC-202011) was authenticated by Professor Shao-Qing Tang (College of Life Science, Guangxi Normal University) and deposited at the State Key Laboratory for Chemistry and Molecular Engineering of Medicinal Resources, Guangxi Normal University.

b. Extraction and Isolation

The dried rattans of *P. championii* (21.0 kg) were soaked for 12 h in 95% aqueous EtOH (100 L) at room temperature, and then extracted three times with 95% aqueous EtOH (3 × 100 L) via refluxing. The filtrate was concentrated under reduced pressure to afford 4.5 kg of crude extract, which was suspended in H₂O and successively partitioned with EtOAc and *n*-BuOH. The EtOAc partition (1.8 kg) was separated via silica gel (200–300 mesh) column chromatography (CC), eluting with a gradient of CH₂Cl₂/MeOH (from 1:0 to 1:1) to give 11 fractions (Frs.1–11).

Fr.6 (20.7 g) was separated via C₁₈ reversed-phase (RP) CC, eluting with a gradient of MeOH-H₂O (30:70 to 70:30) to give 11 subfractions (Frs.6.1–6.11).

Fr.6.2 (656.8 mg) was subjected to Sephadex LH-20 CC (MeOH) to yield six subfractions (Frs.6.2.1–6.2.6). Fr.6.2.5 (183.9 mg) was applied to silica gel (200–300 mesh) CC, eluting with CH₂Cl₂/MeOH (50:1 to 5:1) to obtain nine subfractions (Frs.6.2.5.1–6.2.5.9). Fr.6.2.5.8 (14.3 mg) was further purified using semipreparative RP-HPLC (CH₃CN/H₂O, 22:78, 8.0 mL/min) to afford compound **5** (10.0 mg, *t*_R 37.1 min). Compounds **3** (12.0 mg, *t*_R 38.5 min) and **4** (35.0 mg, *t*_R 42.4 min) were obtained using semipreparative RP-HPLC (CH₃CN/H₂O, 22:78, 8.0 mL/min) from Fr.6.2.5.9 (91.5 mg).

Fr.6.3 (475.2 mg) was separated via a Sephadex LH-20 column, eluting with MeOH to yield six subfractions (Frs.6.3.1–6.3.6). Fr.6.3.5 (223.1 mg) was fractionated using silica gel (200–300 mesh) with gradient elution (CH₂Cl₂/MeOH, 50:1 to 5:1) to provide seven subfractions (Frs.6.3.5.1–6.3.5.7). Purification of Fr.6.3.5.3 (25.4 mg) using semipreparative RP-HPLC (CH₃CN/H₂O, 24:76, 8.0 mL/min) to yield compounds **18** (4.0 mg, *t*_R 54.9 min), **17** (12.0 mg, *t*_R 64.4 min), and **19** (3.0 mg, *t*_R 77.7 min). Fr.6.3.5.4 (93.5 mg) was purified using semipreparative RP-HPLC (CH₃CN/H₂O, 24:76, 8.0 mL/min) to obtain compounds **14** (15.0 mg, *t*_R 48.1 min), **16** (3.0 mg, *t*_R 49.2 min), and **11** (25.0 mg, *t*_R 52.0 min). Fr.6.3.5.5 (32.6 mg) was further purified using semipreparative RP-HPLC (CH₃CN/H₂O, 24:76, 8.0 mL/min) to afford compounds **13** (8.0 mg, *t*_R 40.2 min) and **10** (18.5 mg, *t*_R 44.4 min).

Fr.6.5 (532.6 mg) was separated via Sephadex LH-20 CC (MeOH) and then silica gel (200–300 mesh) CC (CH₂Cl₂/MeOH, 50:1 to 8:1) to provide nine subfractions (Frs.6.5.1–6.5.9). Fr.6.5.3 (15.0 mg) was further purified using semipreparative RP-HPLC (CH₃CN/H₂O, 25:75, 8.0 mL/min) to produce compound **24** (6.0 mg, *t*_R 77.7 min). Fr.6.5.4 (59.0 mg) was chromatographed on a Sephadex LH-20 column using MeOH as a solvent and then purified using semipreparative RP-HPLC (CH₃CN/H₂O, 27:73, 8.0 mL/min) to give compound **22** (3.5 mg, *t*_R 89.4 min). Fr.6.5.5 (35.4 mg) and Fr.6.5.9 (11.9 mg) were further purified using semipreparative RP-HPLC (CH₃CN/H₂O, 27:73, 8.0 mL/min) to produce compounds **23** (11.0 mg, *t*_R 50.0 min) and **2** (3.0 mg, *t*_R 58.1 min), respectively. Further purification of Fr.6.5.6 (26.5 mg) using semipreparative RP-HPLC (CH₃CN/H₂O, 26:74, 8.0 mL/min) yielded compound **15** (7.0 mg, *t*_R 42.9 min). Purification of Fr.6.5.7 (26.5 mg) using semipreparative RP-HPLC (CH₃CN/H₂O, 25:75, 8.0 mL/min) gave compounds **12** (6.0 mg, *t*_R 42.3 min) and **9** (11.0 mg, *t*_R 45.0 min).

Fr.7 (14.0 g) was chromatographed over an MCI-gel column, eluting with MeOH/H₂O (20:80 to 85:15) to give 12 subfractions (Frs.7.1–7.12).

Fr.7.4 (527.6 mg) was fractionated using a silica gel (200–300 mesh) column (CH₂Cl₂/MeOH, 50:1 to 5:1) to obtain seven subfractions (Frs.7.4.1–7.4.7). Fr.7.4.6 (252.4 mg) was purified using semipreparative RP-HPLC (CH₃CN/H₂O, 20:80, 8.0 mL/min) to give compound **1** (80.0 mg, *t*_R 49.1 min).

Fr.7.6 (740.5 mg) was partitioned into six subfractions (Frs.7.6.1–7.6.6) using a Sephadex LH-20 column (MeOH). Fr.7.6.4 (449.3 mg) was separated via silica gel (200–300 mesh) CC to provide eight subfractions (Frs.7.6.4.1–7.6.4.8). Fr.7.6.4.4 (77.3 mg) was further purified using semipreparative RP-HPLC (CH₃CN/H₂O, 24:76, 8.0 mL/min) to yield compound **8** (25.0 mg, *t*_R 39.8 min). Fr.7.6.4.6 (80.6 mg) was purified using semipreparative RP-HPLC (CH₃CN/H₂O, 24:76, 8.0 mL/min) to obtain compounds **7** (30.0 mg, *t*_R 44.1 min) and **6** (8.0 mg, *t*_R 56.2 min).

Fr.7.7 (833.7 mg) was separated using Sephadex LH-20 (MeOH) to obtain eight subfractions (Frs.7.7.1–7.7.8). Fr.7.7.2 (258.5 mg) was then fractionated via silica gel (200–300 mesh) CC to give six subfractions (Frs.7.7.2.1–7.7.2.6). Fr.7.7.2.2 (74.3 mg) and Fr.7.7.2.3 (69.8 mg) were purified using semipreparative RP-HPLC (CH₃CN/H₂O, 27:73, 8.0 mL/min) to yield compounds **21** (25.0 mg, *t_R* 54.4 min) and **20** (35.0 mg, *t_R* 50.2 min), respectively.

c. Physicochemical Properties and Spectroscopic Data of Compounds 1–24

Phaneroside A (**1**): white amorphous powder; $[\alpha]_D^{20} + 33$ (c 0.06, MeOH); UV (MeOH) λ_{\max} (log ϵ) 211 (3.87), 228 (3.92), 314 (4.27) nm; IR (KBr) ν_{\max} 3348, 1696, 1605, 1516, 1171, 1054 cm^{−1}; (+) HRESIMS *m/z* 657.1798 [M + Na]⁺ (calcd for C₃₀H₃₄O₁₅Na, 657.1790); ¹H and ¹³C NMR data, see Tables 1 and 2. All significant data are presented in Supplementary Materials (Figures S1–S9).

Phaneroside B (**2**): white amorphous powder; $[\alpha]_D^{20} + 36$ (c 0.08, MeOH); UV (MeOH) λ_{\max} (log ϵ) 217 (3.95), 320 (4.25) nm; IR (KBr) ν_{\max} 3432, 1696, 1605, 1516, 1271, 1169, 1050 cm^{−1}; (+) HRESIMS *m/z* 641.1847 [M + Na]⁺ (calcd for C₃₀H₃₄O₁₄Na, 641.1841); ¹H and ¹³C NMR data, see Tables 1 and 2. All significant data are presented in Supplementary Materials (Figures S11–S19).

Phaneroside C (**3**): white amorphous powder; $[\alpha]_D^{20} + 22$ (c 0.06, MeOH); UV (MeOH) λ_{\max} (log ϵ) 219 (3.82), 320 (4.10) nm; IR (KBr) ν_{\max} 3417, 1691, 1631, 1605, 1516, 1170, 1052 cm^{−1}; (+) HRESIMS *m/z* 687.1895 [M + Na]⁺ (calcd for C₃₁H₃₆O₁₆Na, 687.1896); ¹H and ¹³C NMR data, see Tables 1 and 2. All significant data are presented in Supplementary Materials (Figures S20–S28).

Phaneroside D (**4**): white amorphous powder; $[\alpha]_D^{20} + 19$ (c 0.06, MeOH); UV (MeOH) λ_{\max} (log ϵ) 231 (3.94), 320 (4.25) nm; IR (KBr) ν_{\max} 3348, 1694, 1632, 1604, 1516, 1270, 1170 cm^{−1}; (+) HRESIMS *m/z* 687.1896 [M + Na]⁺ (calcd for C₃₁H₃₆O₁₆Na, 687.1896); ¹H and ¹³C NMR data, see Tables 1 and 2. All significant data are presented in Supplementary Materials (Figures S29–S37).

Phaneroside E (**5**): white amorphous powder; $[\alpha]_D^{20} + 36$ (c 0.06, MeOH); UV (MeOH) λ_{\max} (log ϵ) 217 (4.07), 237 (4.01), 328 (4.28) nm; IR (KBr) ν_{\max} 3418, 1694, 1606, 1517, 1246, 1170, 1053 cm^{−1}; (+) HRESIMS *m/z* 717.1990 [M + Na]⁺ (calcd for C₃₂H₃₈O₁₇Na, 717.2001); ¹H and ¹³C NMR data, see Tables 1 and 2. All significant data are presented in Supplementary Materials (Figures S38–S46).

Phaneroside F (**6**): white amorphous powder; $[\alpha]_D^{20} + 31$ (c 0.06, MeOH); UV (MeOH) λ_{\max} (log ϵ) 211 (3.86), 228 (3.91), 314 (4.26) nm; IR (KBr) ν_{\max} 3431, 1693, 1605, 1516, 1171, 1051 cm^{−1}; (+) HRESIMS *m/z* 699.1915 [M + Na]⁺ (calcd for C₃₂H₃₆O₁₆Na, 699.1896); ¹H and ¹³C NMR data, see Tables 3 and 5. All significant data are presented in Supplementary Materials (Figures S47–S55).

Phaneroside G (**7**): white amorphous powder; $[\alpha]_D^{20} + 36$ (c 0.06, MeOH); UV (MeOH) λ_{\max} (log ϵ) 211 (3.88), 228 (3.93), 315 (4.28) nm; IR (KBr) ν_{\max} 3421, 1694, 1606, 1516, 1259, 1171, 1059 cm^{−1}; (+) HRESIMS *m/z* 699.1898 [M + Na]⁺ (calcd for C₃₂H₃₆O₁₆Na, 699.1896); ¹H and ¹³C NMR data, see Tables 3 and 5. All significant data are presented in Supplementary Materials (Figures S56–S64).

Phaneroside H (**8**): white amorphous powder; $[\alpha]_D^{20} + 33$ (c 0.06, MeOH); UV (MeOH) λ_{\max} (log ϵ) 211 (3.93), 228 (3.98), 314 (4.32) nm; IR (KBr) ν_{\max} 3326, 1696, 1605, 1516, 1171, 1063 cm^{−1}; (+) HRESIMS *m/z* 699.1899 [M + Na]⁺ (calcd for C₃₂H₃₆O₁₆Na, 699.1896); ¹H and ¹³C NMR data, see Tables 3 and 5. All significant data are presented in Supplementary Materials (Figures S65–S73).

Phaneroside I (**9**): white amorphous powder; $[\alpha]_D^{20} + 23$ (c 0.06, MeOH); UV (MeOH) λ_{\max} (log ϵ) 217 (4.00), 319 (4.29) nm; IR (KBr) ν_{\max} 3427, 1695, 1632, 1605, 1516, 1270, 1170, 1051 cm^{−1}; (+) HRESIMS *m/z* 729.2015 [M + Na]⁺ (calcd for C₃₃H₃₈O₁₇Na, 729.2001); ¹H and ¹³C NMR data, see Tables 3 and 5. All significant data are presented in Supplementary Materials (Figures S74–S82).

Phaneroside J (**10**): white amorphous powder; $[\alpha]_D^{20} + 23$ (c 0.06, MeOH); UV (MeOH) λ_{\max} (log ϵ) 216 (3.98), 320 (4.28) nm; IR (KBr) ν_{\max} 3436, 1691, 1632, 1605, 1516, 1268, 1170 cm^{−1}; (+) HRESIMS *m/z* 729.2012 [M + Na]⁺ (calcd for C₃₃H₃₈O₁₇Na, 729.2001);

^1H and ^{13}C NMR data, see Tables 3 and 5. All significant data are presented in Supplementary Materials (Figures S83–S91).

Phaneroside K (**11**): white amorphous powder; $[\alpha]_D^{20} + 19$ (*c* 0.05, MeOH); UV (MeOH) λ_{max} (log ϵ) 216 (4.01), 319 (4.29) nm; IR (KBr) ν_{max} 3429, 1695, 1632, 1605, 1516, 1268, 1170, 1053 cm^{-1} ; (+) HRESIMS m/z 729.1989 $[\text{M} + \text{Na}]^+$ (calcd for $\text{C}_{33}\text{H}_{38}\text{O}_{17}\text{Na}$, 729.2001); ^1H and ^{13}C NMR data, see Tables 3 and 5. All significant data are presented in Supplementary Materials (Figures S92–S100).

Phaneroside L (**12**): white amorphous powder; $[\alpha]_D^{20} + 19$ (*c* 0.06, MeOH); UV (MeOH) λ_{max} (log ϵ) 218 (4.03), 319 (4.30) nm; IR (KBr) ν_{max} 3436, 1695, 1632, 1605, 1516, 1274, 1171 cm^{-1} ; (+) HRESIMS m/z 729.2018 $[\text{M} + \text{Na}]^+$ (calcd for $\text{C}_{33}\text{H}_{38}\text{O}_{17}\text{Na}$, 729.2001); ^1H and ^{13}C NMR data, see Tables 4 and 5. All significant data are presented in Supplementary Materials (Figures S101–S109).

Phaneroside M (**13**): white amorphous powder; $[\alpha]_D^{20} + 22$ (*c* 0.05, MeOH); UV (MeOH) λ_{max} (log ϵ) 217 (4.04), 319 (4.32) nm; IR (KBr) ν_{max} 3436, 1695, 1632, 1605, 1516, 1268, 1170, 1053 cm^{-1} ; (+) HRESIMS m/z 729.2010 $[\text{M} + \text{Na}]^+$ (calcd for $\text{C}_{33}\text{H}_{38}\text{O}_{17}\text{Na}$, 729.2001); ^1H and ^{13}C NMR data, see Tables 4 and 5. All significant data are presented in Supplementary Materials (Figures S110–S118).

Phaneroside N (**14**): white amorphous powder; $[\alpha]_D^{20} + 28$ (*c* 0.06, MeOH); UV (MeOH) λ_{max} (log ϵ) 232 (4.03), 319 (4.32) nm; IR (KBr) ν_{max} 3432, 1692, 1606, 1518, 1172, 1051 cm^{-1} ; (+) HRESIMS m/z 729.1990 $[\text{M} + \text{Na}]^+$ (calcd for $\text{C}_{33}\text{H}_{38}\text{O}_{17}\text{Na}$, 729.2001); ^1H and ^{13}C NMR data, see Tables 4 and 5. All significant data are presented in Supplementary Materials (Figures S119–S127).

Phaneroside O (**15**): white amorphous powder; $[\alpha]_D^{20} + 22$ (*c* 0.06, MeOH); UV (MeOH) λ_{max} (log ϵ) 217 (4.13), 237 (4.06), 327 (4.34) nm; IR (KBr) ν_{max} 3429, 1695, 1632, 1602, 1516, 1273, 1163, 1051 cm^{-1} ; (+) HRESIMS m/z 759.2124 $[\text{M} + \text{Na}]^+$ (calcd for $\text{C}_{34}\text{H}_{40}\text{O}_{18}\text{Na}$, 759.2107); ^1H and ^{13}C NMR data, see Tables 4 and 5. All significant data are presented in Supplementary Materials (Figures S128–S136).

Phaneroside P (**16**): white amorphous powder; $[\alpha]_D^{20} + 27$ (*c* 0.05, MeOH); UV (MeOH) λ_{max} (log ϵ) 217 (4.22), 236 (4.15), 325 (4.37) nm; IR (KBr) ν_{max} 3432, 1690, 1605, 1517, 1169, 1056 cm^{-1} ; (+) HRESIMS m/z 759.2095 $[\text{M} + \text{Na}]^+$ (calcd for $\text{C}_{34}\text{H}_{40}\text{O}_{18}\text{Na}$, 759.2107); ^1H and ^{13}C NMR data, see Tables 4 and 5. All significant data are presented in Supplementary Materials (Figures S137–S145).

Phaneroside Q (**17**): white amorphous powder; $[\alpha]_D^{20} + 28$ (*c* 0.06, MeOH); UV (MeOH) λ_{max} (log ϵ) 217 (4.07), 237 (4.01), 327 (4.29) nm; IR (KBr) ν_{max} 3426, 1697, 1632, 1598, 1516, 1272, 1161 cm^{-1} ; (+) HRESIMS m/z 759.2097 $[\text{M} + \text{Na}]^+$ (calcd for $\text{C}_{34}\text{H}_{40}\text{O}_{18}\text{Na}$, 759.2107); ^1H and ^{13}C NMR data, see Tables 4 and 5. All significant data are presented in Supplementary Materials (Figures S146–S154).

Phaneroside R (**18**): white amorphous powder; $[\alpha]_D^{20} + 27$ (*c* 0.06, MeOH); UV (MeOH) λ_{max} (log ϵ) 217 (4.13), 234 (4.04), 324 (4.20) nm; IR (KBr) ν_{max} 3428, 1696, 1605, 1517, 1261, 1170, 1054 cm^{-1} ; (+) HRESIMS m/z 759.2096 $[\text{M} + \text{Na}]^+$ (calcd for $\text{C}_{34}\text{H}_{40}\text{O}_{18}\text{Na}$, 759.2107); ^1H and ^{13}C NMR data, see Tables 4 and 5. All significant data are presented in Supplementary Materials (Figures S155–S163).

Phaneroside S (**19**): white amorphous powder; $[\alpha]_D^{20} + 23$ (*c* 0.06, MeOH); UV (MeOH) λ_{max} (log ϵ) 217 (4.17), 235 (4.07), 325 (4.26) nm; IR (KBr) ν_{max} 3397, 2921, 2850, 1646, 1516, 1272 cm^{-1} ; (+) HRESIMS m/z 759.2097 $[\text{M} + \text{Na}]^+$ (calcd for $\text{C}_{34}\text{H}_{40}\text{O}_{18}\text{Na}$, 759.2107); ^1H and ^{13}C NMR data, see Tables 4 and 5. All significant data are presented in Supplementary Materials (Figures S164–S172).

Phaneroside T (**20**): white amorphous powder; $[\alpha]_D^{20} + 25$ (*c* 0.06, MeOH); UV (MeOH) λ_{max} (log ϵ) 211 (3.92), 229 (3.97), 314 (4.32) nm; IR (KBr) ν_{max} 3420, 1697, 1606, 1516, 1262, 1171, 1056 cm^{-1} ; (+) HRESIMS m/z 741.2001 $[\text{M} + \text{Na}]^+$ (calcd for $\text{C}_{34}\text{H}_{38}\text{O}_{17}\text{Na}$, 741.2001); ^1H and ^{13}C NMR data, see Tables 6 and 7. All significant data are presented in Supplementary Materials (Figures S173–S181).

Phaneroside U (**21**): white amorphous powder; $[\alpha]_D^{20} + 26$ (*c* 0.06, MeOH); UV (MeOH) λ_{max} (log ϵ) 211 (3.89), 228 (3.94), 314 (4.28) nm; IR (KBr) ν_{max} 3432, 1695, 1606, 1516, 1170,

1061 cm^{-1} ; (+) HRESIMS m/z 741.2001 $[\text{M} + \text{Na}]^+$ (calcd for $\text{C}_{34}\text{H}_{38}\text{O}_{17}\text{Na}$, 741.2001); ^1H and ^{13}C NMR data, see Tables 6 and 7. All significant data are presented in Supplementary Materials (Figures S182–S190).

Phaneroside V (22): white amorphous powder; $[\alpha]_D^{20} + 26$ (c 0.06, MeOH); UV (MeOH) λ_{max} (log ϵ) 230 (4.02), 316 (4.28) nm; IR (KBr) ν_{max} 3429, 1697, 1606, 1516, 1269, 1170, 1054 cm^{-1} ; (+) HRESIMS m/z 771.2093 $[\text{M} + \text{Na}]^+$ (calcd for $\text{C}_{35}\text{H}_{40}\text{O}_{18}\text{Na}$, 771.2107); ^1H and ^{13}C NMR data, see Tables 6 and 7. All significant data are presented in Supplementary Materials (Figures S191–S199).

Phaneroside W (23): white amorphous powder; $[\alpha]_D^{20} + 23$ (c 0.06, MeOH); UV (MeOH) λ_{max} (log ϵ) 217 (4.04), 319 (4.33) nm; IR (KBr) ν_{max} 3436, 1696, 1633, 1605, 1516, 1268, 1170, 1053 cm^{-1} ; (+) HRESIMS m/z 771.2112 $[\text{M} + \text{Na}]^+$ (calcd for $\text{C}_{35}\text{H}_{40}\text{O}_{18}\text{Na}$, 771.2107); ^1H and ^{13}C NMR data, see Tables 6 and 7. All significant data are presented in Supplementary Materials (Figures S200–S209).

Phaneroside X (24): white amorphous powder; $[\alpha]_D^{20} + 25$ (c 0.06, MeOH); UV (MeOH) λ_{max} (log ϵ) 217 (4.16), 238 (4.10), 328 (4.37) nm; IR (KBr) ν_{max} 3436, 1712, 1633, 1601, 1515, 1273, 1177 cm^{-1} ; (+) HRESIMS m/z 801.2226 $[\text{M} + \text{Na}]^+$ (calcd for $\text{C}_{36}\text{H}_{42}\text{O}_{19}\text{Na}$, 801.2213); ^1H and ^{13}C NMR data, see Tables 6 and 7. All significant data are presented in Supplementary Materials (Figures S210–S217).

d. Acid Hydrolysis of Compound 1

Compound 1 (4.0 mg) was added to 5.0 mL of 9% aqueous HCl in a sealed flask, which was refluxed at 80 °C for 5 h. The acidic aqueous mixture was dried, H_2O (2 mL) was added, and the mixture was extracted with EtOAc (3 \times 2 mL). The aqueous layer was concentrated to obtain the sugar fraction, which was dissolved with MeOH and analyzed using chiral-phase HPLC equipped with a Daicel Chiralpak AD-H column (250 \times 4.6 mm, 5 μm) and an evaporative light-scattering detector (ELSD) using *n*-hexane:EtOH (82:18) as the mobile phase (0.7 mL/min) [27]. The sugars were confirmed to be D-glucose and D-fructose by comparing their retention times with those of D-glucose (17.4 min), L-glucose (18.2 min), D-fructose (25.6 min), and L-fructose (26.4 min) (Figure S10).

e. NO Production Measurements and Cell Viability Assays

The inhibitory effects of the isolated compounds on LPS-stimulated NO production were evaluated using the Griess reaction, and the cytotoxicities of compounds on BV-2 microglial cells were evaluated using MTT assays, as described in our previous report [23]. The result is shown in Figure 7.

f. Antioxidant Activity Assay

The antioxidant activity of the isolated compounds was tested using a DPPH radical scavenging assay as previously described, and vitamin C was used as the positive control [24].

4. Conclusions

In conclusion, 24 new phenylpropanoid esters of sucrose were isolated from the rattans of *P. championii*. Their structures were determined via extensive spectroscopic methods. The configuration of sugar moiety was determined via chiral-phase HPLC equipped with an evaporative light-scattering detector (ELSD) after acid hydrolysis of compound 1. This is the first report of phenylpropanoid esters of sucrose isolated from the family Fabaceae. Structurally, these compounds revealed a huge structural diversity in terms of the number and position of phenylpropanoid and acetyl substituents. Biologically, all the isolated compounds were evaluated for their anti-inflammatory and antioxidant activities, and several compounds showed potent or moderate effects. Additionally, the structure–activity relationship was briefly discussed. These compounds may serve as potential leads for the development of anti-inflammatory agents.

Supplementary Materials: The following supporting information can be downloaded at: <https://www.mdpi.com/article/10.3390/molecules28124767/s1>, Figure S1: UV Spectrum of compound 1. Figure S2: IR (KBr disc) spectrum of compound 1. Figure S3: (+) HRESIMS spectrum of compound 1. Figures S4–S9: 1D and 2D NMR spectra of compound 1. Figure S10: Chiral-HPLC profile from acid hydrolysis of 1 compared to authentic standard. Figure S11: UV spectrum of compound 2. Figure S12: IR (KBr disc) spectrum of compound 2. Figure S13: (+) HRESIMS spectrum of compound 2. Figures S14–S19: 1D and 2D NMR spectra of compound 2. Figure S20: UV spectrum of compound 3. Figure S21: IR (KBr disc) spectrum of compound 3. Figure S22: (+) HRESIMS spectrum of compound 3. Figures S23–S28: 1D and 2D NMR spectra of compound 3. Figure S29: UV spectrum of compound 4. Figure S30: IR (KBr disc) spectrum of compound 4. Figure S31: (+) HRESIMS spectrum of compound 4. Figures S32–S37: 1D and 2D NMR spectra of compound 4. Figure S38: UV spectrum of compound 5. Figure S39: IR (KBr disc) spectrum of compound 5. Figure S40: (+) HRESIMS spectrum of compound 5. Figures S41–S46: 1D and 2D NMR spectra of compound 5. Figure S47: UV spectrum of compound 6. Figure S48: IR (KBr disc) spectrum of compound 6. Figure S49: (+) HRESIMS spectrum of compound 6. Figures S50–S55: 1D and 2D NMR spectra of compound 6. Figure S56: UV spectrum of compound 7. Figure S57: IR (KBr disc) spectrum of compound 7. Figure S58: (+) HRESIMS spectrum of compound 7. Figures S59–S64: 1D and 2D NMR spectra of compound 7. Figure S65: UV spectrum of compound 8. Figure S66: IR (KBr disc) spectrum of compound 8. Figure S67: (+) HRESIMS spectrum of compound 8. Figures S68–S73: 1D and 2D NMR spectra of compound 8. Figure S74: UV spectrum of compound 9. Figure S75: IR (KBr disc) spectrum of compound 9. Figure S76: (+) HRESIMS spectrum of compound 9. Figures S77–S82: 1D and 2D NMR spectra of compound 9. Figure S83: UV spectrum of compound 10. Figure S84: IR (KBr disc) spectrum of compound 10. Figure S85: (+) HRESIMS spectrum of compound 10. Figures S86–S91: 1D and 2D NMR spectra of compound 10. Figure S92: UV spectrum of compound 11. Figure S93: IR (KBr disc) spectrum of compound 11. Figure S94: (+) HRESIMS spectrum of compound 11. Figures S95–S100: 1D and 2D NMR spectra of compound 11. Figure S101: UV spectrum of compound 12. Figure S102: IR (KBr disc) spectrum of compound 12. Figure S103: (+) HRESIMS spectrum of compound 12. Figures S104–S109: 1D and 2D NMR spectra of compound 12. Figure S110: UV spectrum of compound 13. Figure S111: IR (KBr disc) spectrum of compound 13. Figure S112: (+) HRESIMS spectrum of compound 13. Figures S113–S118: 1D and 2D NMR spectra of compound 13. Figure S119: UV spectrum of compound 14. Figure S120: IR (KBr disc) spectrum of compound 14. Figure S121: (+) HRESIMS spectrum of compound 14. Figures S122–S127: 1D and 2D NMR spectra of compound 14. Figure S128: UV spectrum of compound 15. Figure S129: IR (KBr disc) spectrum of compound 15. Figure S130: (+) HRESIMS spectrum of compound 15. Figures S131–S136: 1D and 2D NMR spectra of compound 15. Figure S137: UV spectrum of compound 16. Figure S138: IR (KBr disc) spectrum of compound 16. Figure S139: (+) HRESIMS spectrum of compound 16. Figures S140–S145: 1D and 2D NMR spectra of compound 16. Figure S146: UV spectrum of compound 17. Figure S147: IR (KBr disc) spectrum of compound 17. Figure S148: (+) HRESIMS spectrum of compound 17. Figures S149–S154: 1D and 2D NMR spectra of compound 17. Figure S155: UV spectrum of compound 18. Figure S156: IR (KBr disc) spectrum of compound 18. Figure S157: (+) HRESIMS spectrum of compound 18. Figures S158–S163: 1D and 2D NMR spectra of compound 18. Figure S164: UV spectrum of compound 19. Figure S165: IR (KBr disc) spectrum of compound 19. Figure S166: (+) HRESIMS spectrum of compound 19. Figures S167–S172: 1D and 2D NMR spectra of compound 19. Figure S173: UV spectrum of compound 20. Figure S174: IR (KBr disc) spectrum of compound 20. Figure S175: (+) HRESIMS spectrum of compound 20. Figures S176–S181: 1D and 2D NMR spectra of compound 20. Figure S182: UV spectrum of compound 21. Figure S183: IR (KBr disc) spectrum of compound 21. Figure S184: (+) HRESIMS spectrum of compound 21. Figures S185–S190: 1D and 2D NMR spectra of compound 21. Figure S191: UV spectrum of compound 22. Figure S192: IR (KBr disc) spectrum of compound 22. Figure S193: (+) HRESIMS spectrum of compound 22. Figures S194–S199: 1D and 2D NMR spectra of compound 22. Figure S200: UV spectrum of compound 23. Figure S201: IR (KBr disc) spectrum of compound 23. Figure S202: (+) HRESIMS spectrum of compound 23. Figures S203–S208: 1D and 2D NMR spectra of compound 23. Figure S209: UV spectrum of compound 24. Figure S210: IR (KBr disc) spectrum of compound 24. Figure S211: (+) HRESIMS spectrum of compound 24. Figures S212–S217: 1D and 2D NMR spectra of compound 24.

Author Contributions: D.L. Conceptualization, methodology, validation, and writing—review and editing; Y.-J.H. writing—original draft preparation, chemical experiments, and data curation; Q.L. and B.-J.S. biological experiments. All authors have read and agreed to the published version of the manuscript.

Funding: This work was supported partially by the National Natural Science Foundation of China (22177021 and 81960634).

Institutional Review Board Statement: Not applicable.

Informed Consent Statement: Not applicable.

Data Availability Statement: The data of the article can be obtained from the authors.

Conflicts of Interest: The authors declare no conflict of interest.

Sample Availability: Samples of the compounds are available from the authors.

References

- Zhao, W.; Huang, X.X.; Yu, L.H.; Liu, Q.B.; Li, L.Z.; Sun, Q.; Song, S.J. Tomensides A–D, new antiproliferative phenylpropanoid sucrose esters from *Prunus tomentosa* leaves. *Bioorg. Med. Chem. Lett.* **2014**, *24*, 2459–2462. [\[CrossRef\]](#) [\[PubMed\]](#)
- Vargas, J.A.M.; Ortega, J.O.; Metzker, G.; Larrahondo, J.E.; Boscolo, M. Natural sucrose esters: Perspectives on the chemical and physiological use of an under investigated chemical class of compounds. *Phytochemistry* **2020**, *177*, 112433. [\[CrossRef\]](#) [\[PubMed\]](#)
- Panda, P.; Appalashetti, M.; Judeh, Z.M.A. Phenylpropanoid sucrose esters: Plant-derived natural products as potential leads for new therapeutics. *Curr. Med. Chem.* **2011**, *18*, 3234–3251. [\[CrossRef\]](#)
- Kim, D.; Wang, C.Y.; Hu, R.; Lee, J.Y.; Luu, T.T.T.; Park, H.J.; Lee, S.K. Antitumor activity of vanicoside B isolated from *Persicaria dissitiflora* by targeting CDK8 in triple-negative breast cancer cells. *J. Nat. Prod.* **2019**, *82*, 3140–3149. [\[CrossRef\]](#) [\[PubMed\]](#)
- Panda, P.; Appalashetti, M.; Natarajan, M.; Chan-Park, M.B.; Venkatraman, S.S.; Judeh, Z.M. Synthesis and antitumor activity of lapathoside D and its analogs. *A. Eur. J. Med. Chem.* **2012**, *53*, 1–12. [\[CrossRef\]](#)
- Takasaki, M.; Kuroki, S.; Kozuka, M.; Konoshima, T. New phenylpropanoid esters of sucrose from *Polygonum lapathifolium*. *J. Nat. Prod.* **2001**, *64*, 1305–1308. [\[CrossRef\]](#)
- Chang, C.L.; Zhang, L.J.; Chen, R.Y.; Kuo, L.M.Y.; Huang, J.P.; Huang, H.C.; Lee, K.H.; Wu, Y.C.; Kuo, Y.H. Antioxidant and anti-inflammatory phenylpropanoid derivatives from *Calamus quiquetnerivius*. *J. Nat. Prod.* **2010**, *73*, 1482–1488. [\[CrossRef\]](#)
- Wang, N.; Yao, X.; Ishii, R.; Kitanaka, S. Bioactive sucrose esters from *Bidens parviflora*. *Phytochemistry* **2003**, *62*, 741–746. [\[CrossRef\]](#)
- Zhang, L.; Liao, C.C.; Huang, H.C.; Shen, Y.C.; Yang, L.M.; Kuo, Y.H. Antioxidant phenylpropanoid glycosides from *Smilax bracteata*. *Phytochemistry* **2008**, *69*, 1398–1404. [\[CrossRef\]](#)
- Qian-Cutrone, J.; Huang, S.; Trimble, J.; Li, H.; Lin, P.F.; Alam, M.; Kloor, S.E.; Kadow, K.F. Niruride, a new HIV REV/RRE binding inhibitor from *Phyllanthus niruri*. *J. Nat. Prod.* **1996**, *59*, 196–199. [\[CrossRef\]](#)
- Daude, D.; Remaud-Simeon, M.; Andre, I. Sucrose analogs: An attractive (bio)source for glycodiversification. *Nat. Prod. Rep.* **2012**, *29*, 945–960. [\[CrossRef\]](#) [\[PubMed\]](#)
- Ong, L.L.; Wong, P.W.K.; Raj, S.D.; Khong, D.T.; Panda, P.; Santoso, M.; Judeh, Z.M.A. An orthogonal approach for the precise synthesis of phenylpropanoid sucrose esters. *New J. Chem.* **2022**, *46*, 9710–9717. [\[CrossRef\]](#)
- Montanha, G.S.; Romeu, S.L.Z.; Marques, J.P.R.; Rohr, L.A.; de Almeida, E.; dos Reis, A.R.; Linhares, F.S.; Sabatini, S.; de Carvalho, H.W.P. Microprobe-XRF assessment of nutrient distribution in soybean, cowpea, and kidney bean seeds: A Fabaceae family case study. *ACS Agric. Sci. Technol.* **2022**, *2*, 1318–1324. [\[CrossRef\]](#)
- Maroyi, A. Medicinal uses of the Fabaceae family in Zimbabwe: A review. *Plants* **2023**, *12*, 1255. [\[CrossRef\]](#)
- Wang, M.; Huang, S.; Li, M.; Mckey, D.; Zhang, L. Staminodes influence pollen removal and deposition rates in nectar-rewarding self-incompatible *Phanera yunnanensis* (Caesalpinioideae). *J. Trop. Ecol.* **2019**, *35*, 34–42. [\[CrossRef\]](#)
- Xu, W.; Chu, K.; Li, H.; Zhang, Y.; Zheng, H.; Chen, R.; Chen, L. Ionic liquid-based microwave-assisted extraction of flavonoids from *Bauhinia championii* (Benth.) Benth. *Molecules* **2012**, *17*, 14323–14335. [\[CrossRef\]](#)
- Qin, X.Y.; Luo, J.Y.; Gao, Z.G. *Yao Ethnic Medicinals in China*; Ethnic Publish House: Beijing, China, 2002; p. 57.
- Xu, W.; Huang, M.; Zhang, Y.; Li, H.; Zheng, H.; Yu, L.; Chu, K. Extracts of *Bauhinia championii* (Benth.) Benth. inhibit NF- κ B-signaling in a rat model of collagen-induced arthritis and primary synovial cells. *J. Ethnopharmacol.* **2016**, *185*, 140–146.
- Chen, C.C.; Chen, Y.P.; Hsu, H.Y.; Lee, K.H.; Tani, S.; McPhail, A.T. Bauhinin, a new nitrile glucoside from *Bauhinia championii*. *J. Nat. Prod.* **1985**, *48*, 933–937. [\[CrossRef\]](#)
- Hua, L.P.; Zhang, Y.Q.; Ye, M.; Xu, W.; Wang, X.Y.; Fu, Y.H.; Xu, W. Bioactive dibenzofurans from the rattans of *Bauhinia championii* (Benth.) Benth. *Phytochem. Lett.* **2018**, *24*, 154–157. [\[CrossRef\]](#)
- Hua, L.P.; Zhang, Y.Q.; Ye, M.; Xu, W.; Wang, X.Y.; Fu, Y.H.; Xu, W. A new polyoxygenated abietane diterpenoid from the rattans of *Bauhinia championii* (Benth.) Benth. *Nat. Prod. Res.* **2018**, *32*, 2577–2582. [\[CrossRef\]](#)
- Zhu, F.; Du, B.; Xu, B. Anti-inflammatory effects of phytochemicals from fruits, vegetables, and food legumes: A review. *Crit. Rev. Food Sci.* **2018**, *58*, 1260–1270. [\[CrossRef\]](#) [\[PubMed\]](#)

23. Li, J.; Li, N.; Li, X.; Chen, G.; Wang, C.; Lin, B.; Hou, Y. Characteristic α -acid derivatives from *Humulus lupulus* with antineuroinflammatory activities. *J. Nat. Prod.* **2017**, *80*, 3081–3092. [[CrossRef](#)] [[PubMed](#)]
24. Yang, Z.N.; Su, B.J.; Wang, Y.Q.; Liao, H.B.; Chen, Z.F.; Liang, D. Isolation, absolute configuration, and biological activities of chebolic acid and brevifolincarboxylic acid derivatives from *Euphorbia hirta*. *J. Nat. Prod.* **2020**, *83*, 985–995. [[CrossRef](#)] [[PubMed](#)]
25. Yang, F.; Su, B.J.; Hu, Y.J.; Liu, J.L.; Li, H.; Wang, Y.Q.; Liao, H.B.; Liang, D. Piperhancins A and B, two pairs of antineuroinflammatory cycloneolignane enantiomers from *Piper hancei*. *J. Org. Chem.* **2021**, *86*, 5284–5291. [[CrossRef](#)] [[PubMed](#)]
26. Pan, Q.M.; Li, Y.H.; Hua, J.; Huang, F.P.; Wang, H.S.; Liang, D. Antiviral matrine-type alkaloids from the rhizomes of *Sophora tonkinensis*. *J. Nat. Prod.* **2015**, *78*, 1683–1688. [[CrossRef](#)] [[PubMed](#)]
27. Cao, Y.G.; Ren, Y.J.; Liu, Y.L.; Wang, M.N.; He, C.; Chen, X.; Fan, X.L.; Zhang, Y.L.; Hao, Z.Y.; Li, H.W.; et al. Iridoid glycosides and lignans from the fruits of *Gardenia jasminoides* Eills. *Phytochemistry* **2021**, *190*, 112893. [[CrossRef](#)]

Disclaimer/Publisher’s Note: The statements, opinions and data contained in all publications are solely those of the individual author(s) and contributor(s) and not of MDPI and/or the editor(s). MDPI and/or the editor(s) disclaim responsibility for any injury to people or property resulting from any ideas, methods, instructions or products referred to in the content.